DESIGN OF SERIALLY CONCATENATING TURBO CODING SCHEME FOR FADING CHANNEL AND PERFORMANCE COMPARISON WITH UNCODED AND CONVOLUTIONAL CODING SCHEME

Raj Kumar Goswami
ECE Department, Gayatri Vidya Parishad College of Engineering for Women, Visakhapatnam, India

Abstract: *Whenever a data communication takes place through fading channels, the errors are bounds to occur at the receiving end, primarily because of multipath propagation. There has been a continuous effort from the researchers for designing the Error Correction Schemes which can take care of these errors and ensure that the data received at the receiver end is free of any errors. Especially the efforts have been to design the Forward Error Correction Schemes as these are implemented at the transmitter end itself. These come with the additional cost in terms of expansion of Bandwidth as some bits have to be added for taking care of the error corrections through the implementation of error correction coding. However, there is a coding scheme, that takes care of this aspect, which is known as Trellis Coded Modulation (TCM) Scheme. In TCM the modulation scheme is chosen based on the rate of the convolutional coding scheme. But this coding technique also has its limitations in correcting the number of errors and this led to the development of Turbo Coding, wherein two coders are employed at the transmitter in either serial or parallel configuration and a suitable decoder is designed at the receiver end. In this paper a design of Turbo Coding scheme has been presented which has utilized two convolutional coding schemes i.e., rate 2/3 and rate 3/4 in serially concatenated configuration providing effective rate of 1/2. The performance comparison of designed scheme has been undertaken with both convolutional encoders as well as with the uncoded signal. The modulation scheme that has been utilized is Quadrature Amplitude Modulation. The analysis has been undertaken in MATLAB and it has been observed that the Turbo Coding Scheme provides much better gain in terms of Bit Error Rate (BER) in comparison to the convolutional coding scheme and uncoded data.*

Keywords: Convolutional Code, Fading Channel, TCM, Turbo Code.

1. INTRODUCTION

In any data communication, especially through wireless medium, errors at the receiving end occurs because of the channel through which the data passes through. Some channels introduce less errors, however certain channels where multipath phenomenon is prominent, generally large number of errors occur. Secondly, if the channel utilizes the HF medium then the occurrence of errors is also dependent of time as the channel itself is not stationary. This has led the Electronics and Communication Engineers to find the solution to this problem and many errors correction schemes have been invented since then. There are Block codes, wherein, data is taken block by block, then coded and accordingly at the receiver side same is decoded block by block. This scheme has certain limitations, which gave birth to Convolutional Coding scheme, in which the data is coded in the continuous manner at certain rate. This also had its limitations in terms of increase in the bandwidth post coding and to overcome this problem Trellis Coded Modulation (TCM) was developed by Ungerboeck in 1982 [2]. In TCM, modulation is changed according to the convolutional coding scheme for preserving the bandwidth. For example, suppose 16 QAM is used for modulation and no coding scheme is employed, then four bits are taken at a time for modulation. But if the coding scheme having rate 1/2 is implemented then four bits will become 8 bits indicating that the bandwidth has doubled. In this case if modulation scheme is changed to 256 QAM wherein 8 bits are used for modulation then the bandwidth will be preserved. Here the issue is that if the modulation scheme is changed from 16 QAM to 256 QAM then the distance between the constellation points decreases and therefore the chances of inducing the errors by the channel increase, therefore there has to be a compromise between the rate of coding scheme and modulation technique. This goes to show that there is a limit to which we can preserve the bandwidth post which errors will creep in, which will be impossible to correct. Therefore, in order to overcome this limitation and to ensure that more errors are corrected, Turbo Coding was introduced by Berrou et al in 1993 [3]. The performance of coding scheme is judged from the point of Bit Error Rate (BER), which indicates the number of bits in error vis-s-vis the number of bits transmitted.

At the transmitter end Turbo Coding scheme employs two encoders which are concatenated, either in series or in parallel configuration along with an interleaver, which randomize the bits before giving as input to the second decoder. These are designated as Serially Concatenated Convolutional Codes (SCCC) and Parallel Concatenated Convolutional Codes (PCCC). The configuration of these encoders is shown in Fig 1 and Fig 2 respectively.

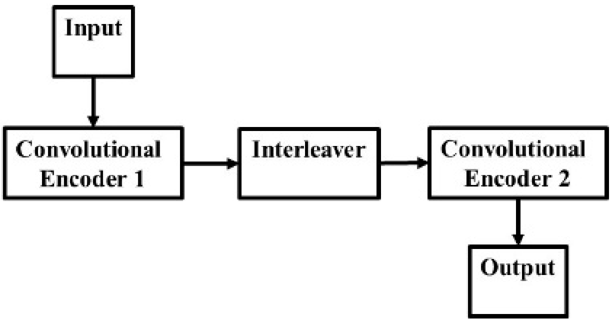

Fig. 1 SCCC Encoder

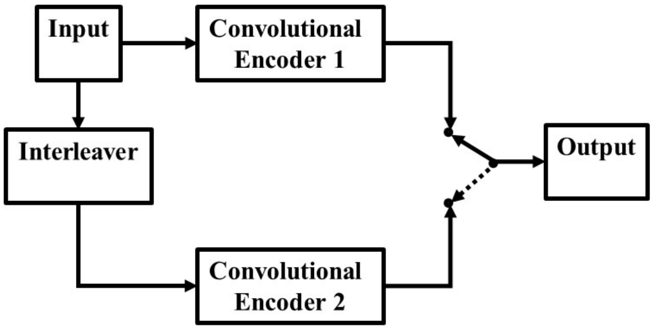

Fig. 2 PCCC Encoder

For the purpose of decoding at the receiver, APP decoders have been utilized, for decoding the Turbo encoding scheme in respect of both the configuration albeit with the slight change in configuration as shown in Fig 3 and Fig 4 respectively for SCCC and PCCC. In both the cases the output of first decoder is given to the second decoder through interleaver and output of second decoder is fed to the first decoder through the interleaver. This iteration of decoding continues till the error reduces to the desired level and that is the point the output of second decoder is considered as the output of the Turbo decoder.

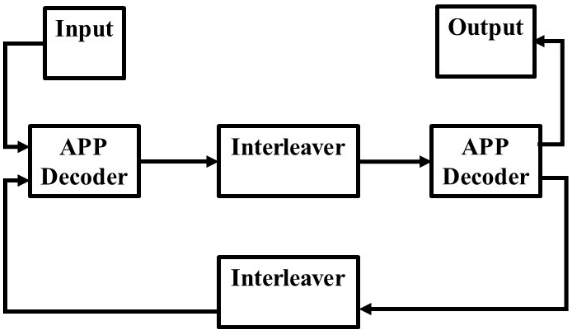

Fig. 3 SCCC Decoder

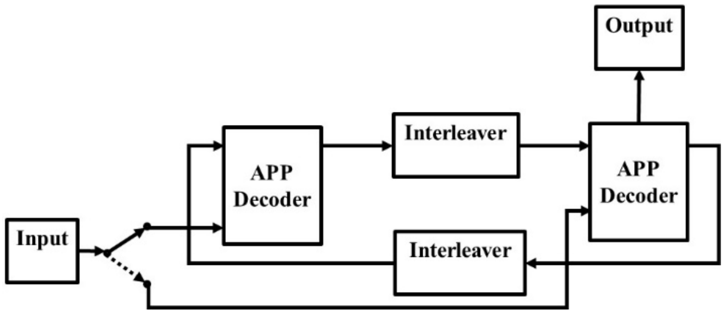

Fig. 4 PCCC Decoder

General Block diagram of communication system is shown in Fig 5. The channel that has been considered here, is the fading channel [9].

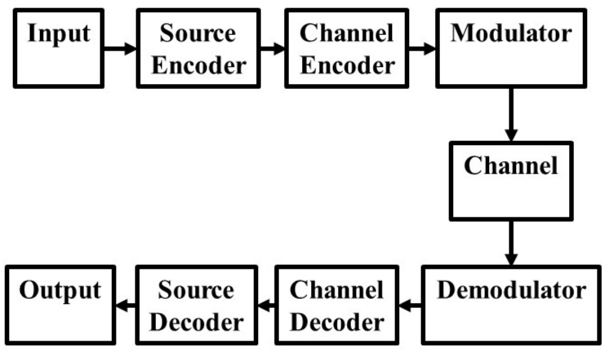

Fig. 5 Communication System block diagram

Source Coding is primarily used for removing the redundant information. The examples of source coding are compression schemes like zip, rar etc. After source coding, Channel coding is undertaken and it is in the channel coding, the Forward Error Correction (FEC) schemes are implemented. Post implementation of FEC, the bits are given as input to the modulator for modulation and finally after modulation, the data is transmitted to the channel. In the present case, the modulation scheme chosen is QAM therefore the output of the Channel Encoder is arranged in the vector form where each vector represents a point in the complex plane pertaining to the specific QAM architecture.

At receiver, the received data will be corrupted as it has passed through the fading channel. The sequence $r_l = (r_1, r_2, \ldots r_l)$ after demodulating is fed to the decoder which performs the decoding. The block diagram of the receiver at the baseband level has been shown in Fig. 6.

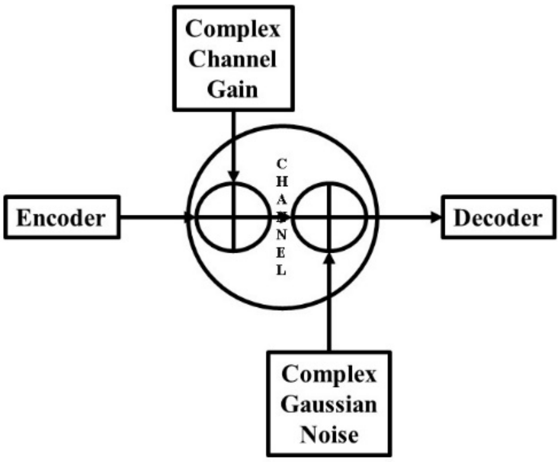

Fig. 6 Block Diagram of Baseband Receiver.

From the receiver diagram the received signal at time *i* can be written as

$$r_i = c_i . s_i + n_i \qquad (1)$$

where n_i indicates the zero-mean complex Gaussian noise with variance $\sigma^2_n = N_0/2$ and c_i is the complex channel gain of a complex Gaussian process with variance σ^2_c.
The complex channel gain c_i can also be expressed as phasor

$$c_i = a_i \cdot e^{j\phi_i} \qquad (2)$$

where, a_i and ϕ_i represent the amplitude and phase respectively.

Here it has been assumed that the receiver undertakes the coherent detection, implying that the channel phase shift has been compensated by the receiver, therefore (1) can be further simplified as

$$r_i = a_i s_i + n_i \qquad (3)$$

The fading aspect here is defined by a_i. When there is no line-of-sight path and there is only a diffused multipath component, the a_i is usually modeled as Rayleigh fading channel, whose probability density function (PDF) is defined as

$$p_A(a) = 2ae^{-a^2}, \qquad a \geq 0. \qquad (4)$$

And when in addition to the multipath components there is a single dominant, nonfading component i.e., when both transmitter and receiver are in line of sight then in such a scenario, the channel is modeled as Rician Fading Channel with a PDF as given below

$$p_A(a) = 2a(1+K)e^{-(K+a^2(1+K))} I_0(2a\sqrt{K(1+K)}), \quad a \geq 0 \quad (5)$$

where the Rician parameter K is the ratio of the received signal in the direct and diffused multipath components and $I_0(.)$ is the zero-order modified Bessel function of the first kind. Here important point to remember is that probability density function has to be normalized in order to represent the average signal energy per channel symbol, E_s. In this paper Rician Channel has been considered and the effect of time-varying multipath has been neglected. This assumption is appropriate here as the receiver will employ equalization techniques for taking care of this aspect.

2. PERFORMANCE ANALYSIS

The performance analysis has been undertaken with the assumption that the fading amplitudes are statistically independent and the channel is memoryless. Error event probability will determine the performance of the design i.e., if the probability of error event is less, then the errors will be less and vice-versa. In this section the error event probability will be derived. Let us look at the upper bound of the pairwise error probability [9]. If the detection is considered to be coherent, CSI is perfect and the fading is independent from symbol to symbol then the upper bound of the pairwise error probability of decoding the symbol sequence as $\hat{s}_l$ when the transmitted symbol sequence is s_l in respect of Rician Channel is given as

$$P_2(s_l, \hat{s}_l) \leq \prod_{i=1}^{l} \frac{1+K}{1+K+\frac{1}{4N_0}|s_i - \hat{s}_i|^2} \exp\left[-\frac{K\frac{1}{4N_0}|s_i - \hat{s}_i|^2}{1+K+\frac{1}{4N_0}|s_i - \hat{s}_i|^2} \right] \quad (6)$$

Now when the Signal to Noise Ratio is high the above equation simplifies to

$$P_2(s_l, \hat{s}_l) \leq \prod_{i \in \eta} \frac{(1+K)e^{-K}}{\frac{1}{4N_0}|s_i - \hat{s}_i|^2} \quad (7)$$

where η indicates only those values of i where s_i is not equal to $\hat{s}_i$. Now if these number of values is represented by l_η, then (7) can be rewritten as follows. l_η is also known as the effective length of the error event $(s_l, \hat{s}_l)$.

$$P_2(s_1, \hat{s}_1) \leq \frac{((1+K)e^{-K})^{l_\eta}}{\left(\frac{1}{4N_0}\right)^{l_\eta} d_P^2(l_\eta)} \quad (8)$$

where $d_P^2(l_\eta)$ is the squared product distance of the signals when s_i is not equal to $\hat{s}_i$, along the error event $(s_l, \hat{s}_l)$ path and is defined as

$$d_P^2(l_\eta) = \prod_{i \in \eta} |s_i - \hat{s}_i|^2 \quad (9)$$

An error event is one where the path of received data is deviated from the intended one i.e., not observed in accordance with the designed one. The same has been depicted in Fig. 7. It can be seen that the designed/ intended path is s_1, s_2 till s_l, whereas the path traced by the received symbols is $\hat{s}_1$, $\hat{s}_2$, till $\hat{s}_l$.

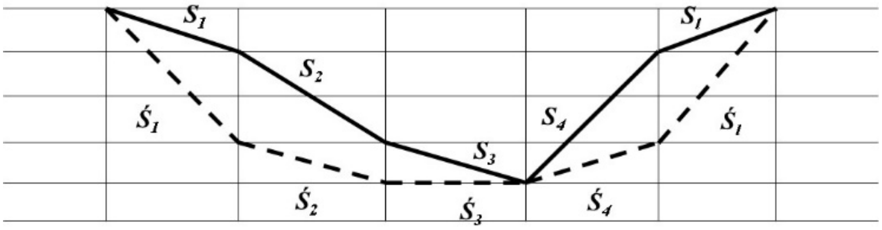

Fig. 7 Error event considering length as l.

Now, if we sum all error event probabilities over l, l=1…∞, by taking all transmitted sequences into consideration, an upper bound can be calculated, which can be written as follows

$$P_e \leq \sum_{l=1}^{\infty} \sum_{s_l} \sum_{\hat{s}_l \neq s_l} P(s_l) P_2(s_l, \hat{s}_l) \qquad (10)$$

where $P(\boldsymbol{s}_l)$ is the *a priori* probability of transmitting symbol $\boldsymbol{s}_l$. $P_2(s_l, \hat{s}_l)$ in the above equation can be substituted at high SNR's by (8) and therefore the upper bound in respect of a Rician fading channel can be written as

$$P_e \leq \sum_{l_\eta} \sum_{d_P^2(l_\eta)} \alpha(l_\eta, d_P^2(l_\eta)) \frac{((1+K)e^{-K})^{l_\eta}}{\left(\frac{1}{4N_0}\right)^{l_\eta} d_P^2(l_\eta)} \qquad (11)$$

Here, the average number of code sequences having the effective length l_η has been indicated by $\alpha(l_\eta, d_p^2(l_\eta))$ and the squared product distance has been indicated by $d_p^2(l_\eta)$. It can be observed from (11) that at high SNR, the error event is dominated by smallest effective length l_η and the smallest product distance $d_p^2(l_\eta)$. Therefore, in order to simplify further $\min(l_\eta)$ is denoted by L, which can be called as effective length of the code and the corresponding squared product distance by $d_p^2(L)$, then the error event probability can be approximated as follows

$$P_e \approx \alpha(L, d_P^2(L)) \frac{((1+K)e^{-K})^{L}}{\left(\frac{1}{4N_0}\right)^{L} d_P^2(L)} \qquad (12)$$

In respect of Rayleigh fading channel, where K is equal to zero (12) can be further simplifies as

$$P_e \approx \frac{\alpha(L, d_P^2(L))}{\left(\frac{1}{4N_0}\right)^{L} d_P^2(L)} \qquad (13)$$

And in respect of AWGN channel, where K is equal to ∞, the P_e can be shown as follows [9]

$$P_e \approx \frac{1}{2} N(d_{free}) erfc\left(\sqrt{\frac{d_{free}^2}{4N_0}}\right) \qquad (14)$$

where d_{free} is the free Euclidean distance of the code.

In this paper the performance analysis has been undertaken in respect of Rician Fading Channel and therefore only equation (12) is relevant, other two cases have been just indicated as special cases, where K is either zero or infinity. The turbo coding scheme that has been used in this paper is serially concatenated convolutional coding (SCCC) scheme [13]. Where two convolutional encoders having rates 2/3 and rate 3/4 have been used in serial configuration providing the effective rate of 1/2. Performance analysis has been undertaken for both convolutional coding schemes and the turbo coding scheme along with the uncoded data as well for the purpose of comparison. It is to be noted that both encoders play the important roles in the performance of SCCC [10]. The decoding is undertaken iteratively, soft output of one decoder is fed to the other decoder and the soft output of second decoder is fed back to the first decoder as input [11] and this process continues till the decoding is complete. When it comes to complexity, it is more or less equal to the complexity of Convolutional Code. In this paper APP algorithm has been used in decoder [12].

3. DESIGN OF ENCODERS

In the designing of encoder, as discussed above two convolutional encoders have been utilized in serial configuration along with an interleaver whose input is the output of first encoder and after interleaving serves as input to the second encoder. The convolutional encoders those have been used have Rates 2/3 and 3/4 and states 8 and 16 respectively. Ungerboeck has designed a rate 2/3, 8-state, 8-PSK TCM that provides an effective length, L, of 2 and $d^2_{free} = 4.586E_s$, which was optimized for the AWGN channel [3]. In the present case, common rules have been utilized for designing both encoders optimized for fading channel [15]and are as follows.

The signals associated with transitions between states of consecutive stages are represented by a matrix M of dimension 8 x 8, in case of Rate 2/3 and 16 x 16 in case of rate 3/4, whose ij^{th} element represents the signal associated with the path from state i, at stage k, to state j, at stage $k+1$, of the trellis. Also, the elements of the i^{th} row indicate signals associated with path diverging from state i and the elements of the j^{th} column show signals associated with paths reemerging at state j. Using set partitioning, the 8 QAM and 16 QAM signal set can be partitioned into two subsets, having alternate symbols in each subset. i.e., s_0, s_2, s_4, s_6 …….in subset 1 and s_1, s_3, s_5, s_7 …. in subset 2. To assign signal points to the elements of matrix ***M***, the following rules have been proposed: -

a. In a given row or column, a signal can occur only once.

b. As the number of paths emerging from a state are 4 in case of rate 2/3 code and 8 in case of rate 3/4, and there are 8 states in case of rate 2/3 code and 16 in case of rate 3/4, all transitions are not possible. Therefore the rule which is followed is that a signal can be associated with a transition path between two states, only if the LSB of the the initial state is the same bit, $z \in \{0,1\}$, as the MSB of the destination state [15].

c. The distance between a pair of signals associated with a given row or a column is δ_1 or δ_3, as shown in the schematic diagram shown in Fig. 9 in case of rate 2/3.

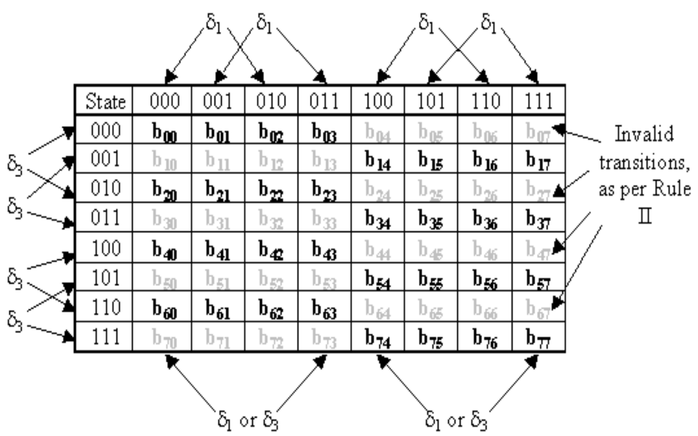

Fig. 9 The schematic representation of Rule 'b' and Rule 'c'

Rule 'a' ensures that the effective length of the code is maximum whereas Rule 'b' ensures that the distances between each pair of diverging paths from state i and the distances between each pair of converging paths to state j are at least δ_1. The state transitions for the proposed encoder in respect of rate 3/4 have been shown in Table I.

Table I. State transitions

State	0000	0001	0010	0011	0100	0101	0110	0111	1000	1001	1010	1011	1100	1101	1110	1111
0000	**s_{00}**	**s_{01}**	**s_{02}**	**s_{03}**	**s_{04}**	**s_{05}**	**s_{06}**	**s_{07}**	s_{08}	s_{09}	s_{0A}	s_{0B}	s_{0C}	s_{0D}	s_{0E}	s_{0F}
0001	s_{10}	s_{11}	s_{12}	s_{13}	s_{14}	s_{15}	s_{16}	s_{17}	**s_{18}**	**s_{19}**	**s_{1A}**	**s_{1B}**	**s_{1C}**	**s_{1D}**	**s_{1E}**	**s_{1F}**
0010	**s_{20}**	**s_{21}**	**s_{22}**	**s_{23}**	**s_{24}**	**s_{25}**	**s_{26}**	**s_{27}**	s_{28}	s_{29}	s_{2A}	s_{2B}	s_{2C}	s_{2D}	s_{2E}	s_{2F}
0011	s_{30}	s_{31}	s_{32}	s_{33}	s_{34}	s_{35}	s_{36}	s_{37}	**s_{38}**	**s_{39}**	**s_{3A}**	**s_{3B}**	**s_{3C}**	**s_{3D}**	**s_{3E}**	**s_{3F}**
0100	**s_{40}**	**s_{41}**	**s_{42}**	**s_{43}**	**s_{44}**	**s_{45}**	**s_{46}**	**s_{47}**	s_{48}	s_{49}	s_{4A}	s_{4B}	s_{4C}	s_{4D}	s_{4E}	s_{4F}
0101	s_{50}	s_{51}	s_{52}	s_{53}	s_{54}	s_{55}	s_{56}	s_{57}	**s_{58}**	**s_{59}**	**s_{5A}**	**s_{5B}**	**s_{5C}**	**s_{5D}**	**s_{5E}**	**s_{5F}**
0110	**s_{60}**	**s_{61}**	**s_{62}**	**s_{63}**	**s_{64}**	**s_{65}**	**s_{66}**	**s_{67}**	s_{68}	s_{69}	s_{6A}	s_{6B}	s_{6C}	s_{6D}	s_{6E}	s_{6F}
0111	s_{70}	s_{71}	s_{72}	s_{73}	s_{74}	s_{75}	s_{76}	s_{77}	**s_{78}**	**s_{79}**	**s_{7A}**	**s_{7B}**	**s_{7C}**	**s_{7D}**	**s_{7E}**	**s_{7F}**
0000	**s_{80}**	**s_{81}**	**s_{82}**	**s_{83}**	**s_{84}**	**s_{85}**	**s_{86}**	**s_{87}**	s_{88}	s_{89}	s_{8A}	s_{8B}	s_{8C}	s_{8D}	s_{8E}	s_{8F}
1001	s_{90}	s_{91}	s_{92}	s_{93}	s_{94}	s_{95}	s_{96}	s_{97}	**s_{98}**	**s_{99}**	**s_{9A}**	**s_{9B}**	**s_{9C}**	**s_{9D}**	**s_{9E}**	**s_{9F}**
1010	**s_{A0}**	**s_{A1}**	**s_{A2}**	**s_{A3}**	**s_{A4}**	**s_{A5}**	**s_{A6}**	**s_{A7}**	s_{A8}	s_{A9}	s_{AA}	s_{AB}	s_{AC}	s_{AD}	s_{AE}	s_{AF}
1011	s_{B0}	s_{B1}	s_{B2}	s_{B3}	s_{B4}	s_{B5}	s_{B6}	s_{B7}	**s_{B8}**	**s_{B9}**	**s_{BA}**	**s_{BB}**	**s_{BC}**	**s_{BD}**	**s_{BE}**	**s_{BF}**
1100	**s_{C0}**	**s_{C1}**	**s_{C2}**	**s_{C3}**	**s_{C4}**	**s_{C5}**	**s_{C6}**	**s_{C7}**	s_{C8}	s_{C9}	s_{CA}	s_{CB}	s_{CC}	s_{CD}	s_{CE}	s_{CF}
1101	s_{D0}	s_{D1}	s_{D2}	s_{D3}	s_{D4}	s_{D5}	s_{D6}	s_{D7}	**s_{D8}**	**s_{D9}**	**s_{DA}**	**s_{DB}**	**s_{DC}**	**s_{DD}**	**s_{DE}**	**s_{DF}**
1110	**s_{E0}**	**s_{E1}**	**s_{E2}**	**s_{E3}**	**s_{E4}**	**s_{E5}**	**s_{E6}**	**s_{E7}**	s_{E8}	s_{E9}	s_{EA}	s_{EB}	s_{EC}	s_{ED}	s_{EF}	s_{6F}
1111	s_{F0}	s_{F1}	s_{F2}	s_{F3}	s_{F4}	s_{F5}	s_{F6}	s_{F7}	**s_{F8}**	**s_{F9}**	**s_{FA}**	**s_{FB}**	**s_{FC}**	**s_{FD}**	**s_{FE}**	**s_{FF}**

Set partitioning [16] in respect of 16-QAM signal set is partitioned as shown in Fig. 11, the 16-QAM signal set has been partitioned into two subsets, viz., $A_0 = \{s_0,s_2,s_4,s_6,s_8,s_{10},s_{12},s_{14}\}$ and $A_1 = \{s_1,s_3,s_5,s_7,s_9,s_{11},s_{13},s_{15}\}$ with minimum intra-set distance.

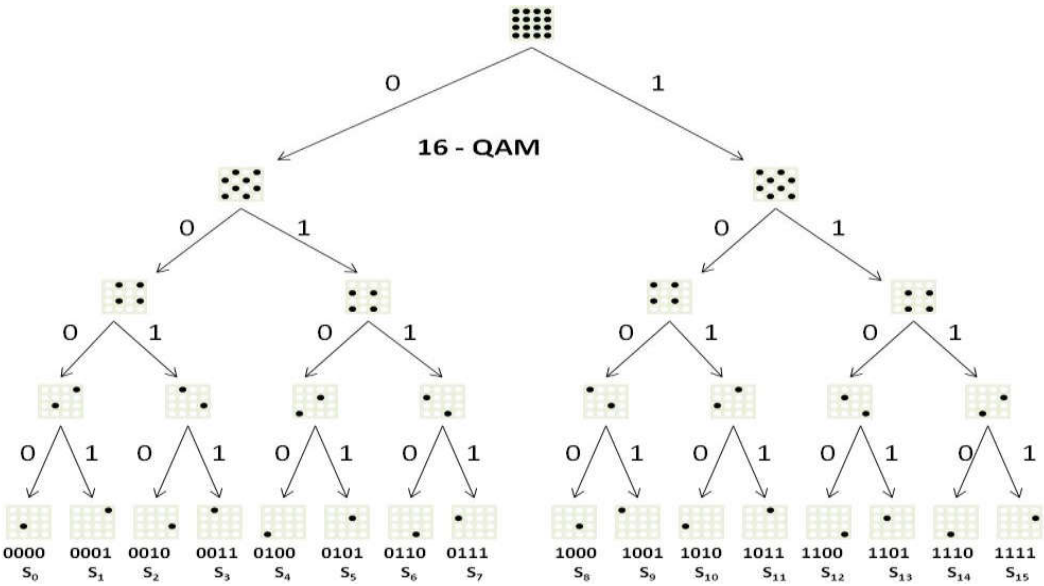

Fig. 11 Set partitioning

The trellis diagram in respect of rate 3/4 construction is shown in Fig. 12.

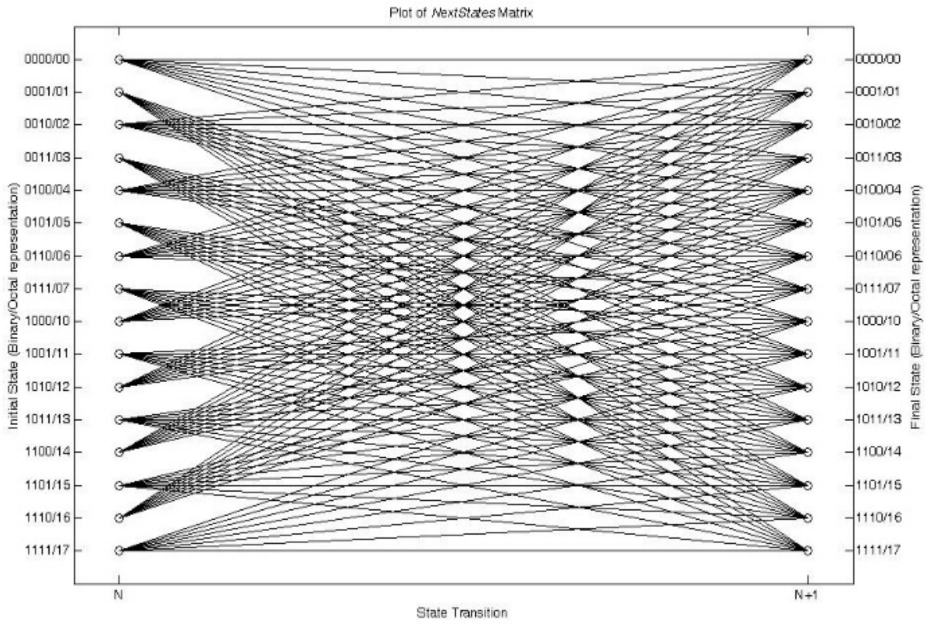

Fig. 13 Trellis diagram of the rate 3/4, 16-state, 16 QAM

4. SIMULATION AND RESULTS

In the Fig 14 overall block diagram of the simulation is shown wherein each block and its functions has been specified. In the simulation Bernoulli Binary generator has been used as the source of random input bits, the output of this source is fed into the four programs namely, uncoded, convolutional code having rate 2/3, convolutional code having rate 3/4 and hybrid code of rate 1/2 involving wherein both convolutional encoders are concatenated in series separated by an interleaver as shown in fig. 15. The uncoded and encoded data is then fed to the QPSK, 8-QAM and 16 QAM Modulators. Subsequently, their outputs are fed into a multipath Rician fading channel.

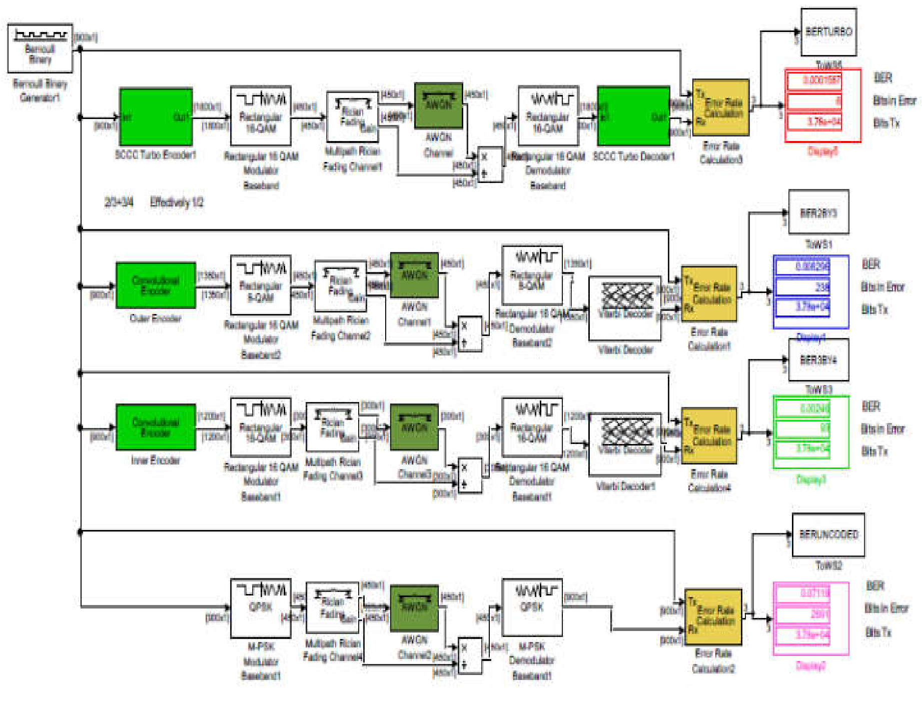

Fig. 14 Block Diagram of Simulation

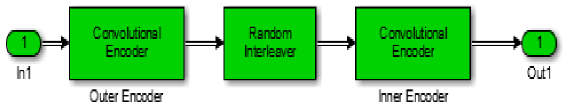

Fig. 15 Diagram of Turbo Decoder

At the receiver, signal is initially demodulated using 16-QAM, 8-QAM and QPSK demodulators and then fed into the respective decoders. The turbo decoder contains two decoders connected serially and separated by an interleaver as shown in Fig. 16.

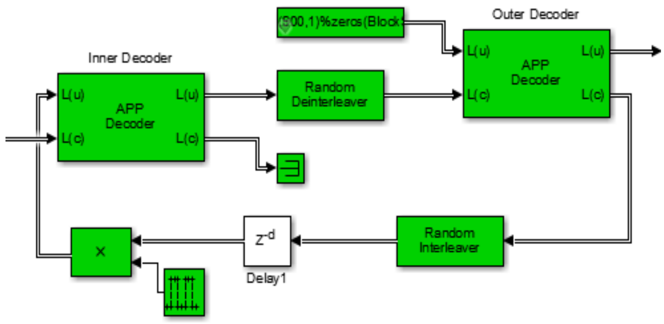

Fig. 16 Diagram of Turbo Decoder

Finally, the performance of the proposed hybrid turbo coding scheme has been evaluated in terms of the bit error rate in respect of Rician channel. The BER of proposed Hybrid Turbo Scheme in respect of Rician channel has been shown in Fig. 17. The BER has also been compared with the BERs achieved in respect of convolutional encoders of rate 2/3 and 3/4. The plot also shows the BER of the uncoded QPSK scheme for the purpose of comparison.

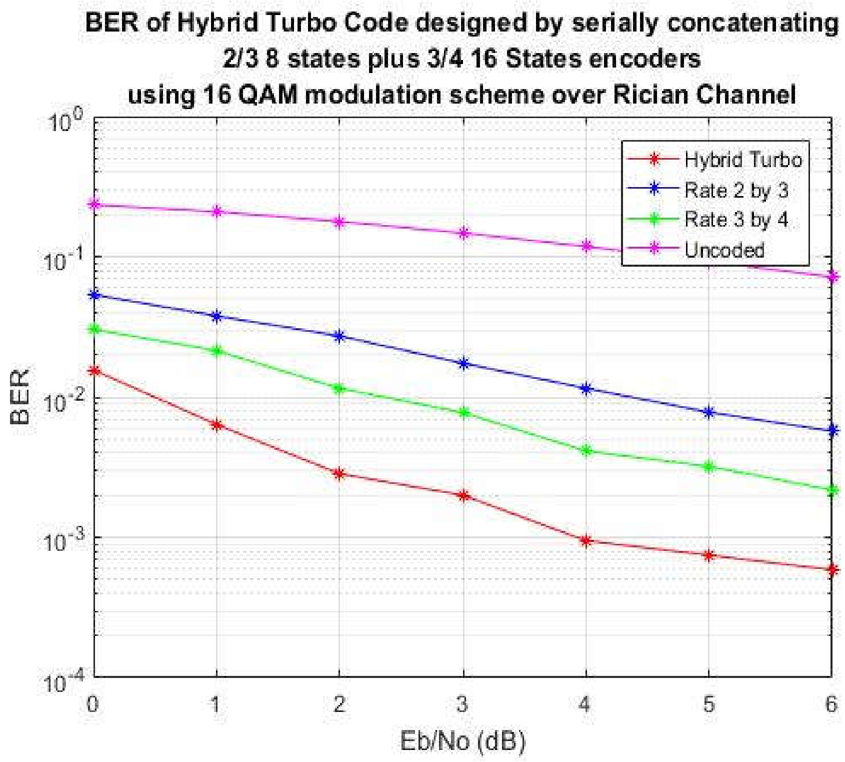

Fig. 17 Performance analysis of the proposed Hybrid Turbo Coding scheme in Rician Environment

5. CONCLUSION

In this paper, design of Hybrid Turbo Coding Scheme based on Serially Concatenating two convolutional encoders having Rates 2/3 and 3/4 has been explored in respect of Rician Channel. The convolutional coders, which forms the integral part of Turbo Code, has been designed in respect of fading channel. The performance analysis has been undertaken in respect of Rician fading environment. For the purpose of comparison, the analysis has also been undertaken in respect of both constituent encoders and the results have been compared along with the results of uncoded data. The simulation results show that in the case of Rician fading environment, the proposed Hybrid Turbo coding scheme provides coding gain of more than 3 dB with respect to the TCM scheme used by the constituent encoders. The analysis had been done on similar work [17], [18], though not on the exact work that has been proposed in this paper; however, the same can be compared to some extent. The simulated results have shown that the proposed scheme performs better.

[1] *http://en.wikipedia.org/wiki/Forward_error_correction*

[2] *G. Ungerboeck, "Channel coding with multilevel phase signaling", IEEE Trans. Inf. Th., vol.IT-25, Jan. 1982, pp.55-67.*

[3] *C. Berrou, A. Glavieux, and P. Thitimajshima, "Near Shannon limit error-correcting coding and decoding: Turbo-codes", Proc. Int. Conf. Communications, Geneva, Switzerland, May 1993, pp. 1064–1070.*

[4] *http://en.wikipedia.org/wiki/Turbo_code*

[5] *L. Hanzo, T. H. Liew, B. L. Yeap. Turbo Coding, Turbo Equalisation and Space-Time Coding for Transmission over Fading Channels, Wiley-IEEE Press May 2003.*

[6] *S. Benedetto, D. Divsalar, G. Montorsi, and F. Pollara, "Serial concatenation of interleaved codes: Performance analysis, design and iterative decoding", IEEE Trans. Inform. Theory, vol. 44, May 1998, pp. 909–926,*

[7] *Raffi Achiba and Mehrnaz Mortazavi, "Turbo Codes Performance and Design Trade Offs", MILCOM 2000, PP 174-180*

[8] *Keattisak, Sripimanwat, Turbo code Applications, Springer 2005.*

[9] *Jamali Hamidreza S. and Tho Le Ngoc, Coded Modulation Techniques for Fading Channels, Boston: Kluwer Academic Publishers, 1994.*

[10] *L. Hanzo, T.H. Liew, B.L. Yeap Turbo Coding, Turbo Equalisation and Space-Time Coding, John Wiley & Sons, Ltd. 2002*

[11] *Rui Xue, Dan-Feng, Zhao Jie Zhang, "An Improved Method for the Convergence of Iterative Detection in SCCC System" Wireless Communications, Networking and Mobile Computing, 2008. 12-14 Oct. 2008 pp1-5*

[12] *S. Benedetto, D. Divsalar, G. Montorsi and F. Pollara, "A Soft-Input Soft-Output APP Module for Iterative Decoding of Concatenated Codes", IEEE communications letters, VOL. 1, NO. 1, January 1997 pp 22 – 24*

[13] *G. D. Forney, Concatenated Codes, MIT Press, Cambridge, MA, 1966.*

[14] *J. Du and B. Vucetic, "New M-PSK Trellis Codes for fading channels," Electronics Letters, Vol. 26, No.16, pp. 1267-1269, Aug. 1990.*

[15] *Rajkumar Goswami, SasiBhusana Rao, Rajan Babu, Ravindra Babu, "8 State Rate 2/3 TCM Code Design for Fading Channel" IEEE conference On Control, Communications and Automation, Dec 2008,Vol-II, pp. 323 -326.*

[16] *Dariush Divsalar and Marvin K. Simon, "The Design of Trellis Coded MPSK for Fading Channels: Set Partitioning for Optimum Code Design," IEEE Trans. on Communications, Sept. 1988, Vol. 36, No. 9, pp. 1013-1021,*

[17] *Juihong Yuan, B Vucetic and Wen Feng, "Turbo-Coded M-QAM for fading channel", Electronic Letters, 31 Aug 2000, Vol. 36 No 18, pp 1562 – 1503*

[18] *Manjeet Singh, Ian Wassell, "Comparison between Serial and Parallel Concatenated Channel Coding Schemes using Continuous Phase Modulation over AWGN and Fading Channels", CIC 2001, Las Vegas, June 2001.*